Int J Adv Manuf Technol (2009) 42:30–40
DOI 10.1007/s00170-008-1582-6

ORIGINAL ARTICLE

A comparative study of the tool–chip contact length in turning of two engineering alloys for a wide range of cutting speeds

S. A. Iqbal · P. T. Mativenga · M. A. Sheikh

Received: 8 February 2008 / Accepted: 21 May 2008 / Published online: 11 July 2008

Abstract Tool chip contact length is an important parameter in machining, as it provides an indication of the size of area of interaction between the hot chip and the tool surface and hence the interface heat transfer zone. Heat transfer and thermally activated wear modes usually dominate tool wear in the high speed machining of steels and machining of titanium alloys at most cutting speeds. In this study, existing models for the prediction of tool–chip contact length are reviewed and examined for their suitability in high speed machining of two widely used engineering alloys. Orthogonal turning tests for AISI 1045 steel and Ti6Al4V titanium alloy are conducted for a range of cutting speeds from conventional to high speeds. New contact length models are presented for both materials covering a wide range of cutting speeds. More significantly, these contact length models are appropriate for high speed machining where thermal loads significantly influence process performance. Additionally, the work discusses how the machinability of engineering materials influences the ability to predict contact length.

Keywords High speed machining (HSM) · Contact length models · Dimensional analysis

List of Symbols

h_1	Undeformed chip thickness (mm)
h_2	Chip thickness (mm)
L_c	Contact length (mm)
n	Material constant
V_c	Cutting velocity (m/min)
α	Rake angle (degree)
θ	Inclination of resultant force with shear plane (degree)
λ	Chip compression ratio
ϕ	Shear angle (degree)

S. A. Iqbal (✉) · P. T. Mativenga · M. A. Sheikh
Manufacturing and Laser Processing Research Group,
School of Mechanical, Aerospace and Civil Engineering,
The University of Manchester,
Manchester, UK
e-mail: amir.syed@postgrad.manchester.ac.uk

1 Introduction

1.1 High speed machining

High speed machining (HSM) can be considered as machining at significantly higher cutting speeds and feed rates compared to conventional practice which has also been defined by other authors using various criteria [1, 2]. The most popular definition of these is the one according to the workpiece material as shown in Fig. 1. HSM provides the opportunity to use optimum cutting parameters for obtaining high production rates. Other benefits reported for HSM include the ability for direct machining of hardened materials, lower cutting forces and possibility for improving surface finish [3]. The machining technology has gained considerable success during the last few years in several sectors due to the above advantages. However, much of the knowledge in this field is still acquired empirically, and the modelling of the process is relatively undeveloped [4].

In HSM, the chip formation process occurs at a very high strain rate and nonlinear plastic deformation of the workpiece material in the contact area. This generates localised stresses in the cutting tool and a sharp rise in the temperature at the interface. In addition, it has been established that the process of plastic deformation in the primary shear zone depends upon the condition of the

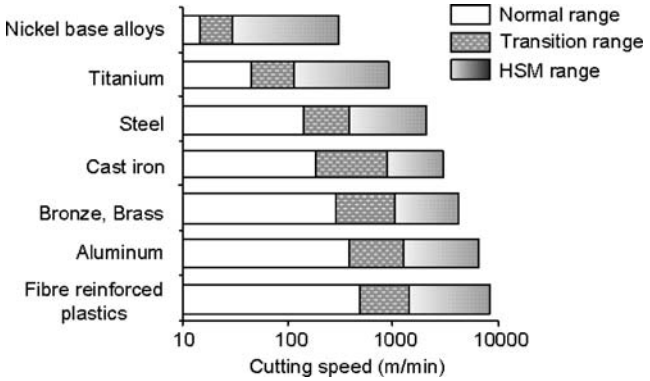

Fig. 1 Cutting speed regimes for high speed machining [1]

sliding of the chip along the tool face. It is important, therefore, to investigate the contact zone after the chip is separated from the workpiece [5].

AISI 1045 carbon steel and Ti6Al4V titanium alloy are selected for the present investigation. These two workpiece materials cover a broad spectrum of engineering applications. AISI 1045 steel is a typical material for a variety of automobile components such as crankshafts, piston rods, steering components, axles, gears, etc. and is also used for the manufacturing of rails, railway wheels and rail axles. It has excellent performance in die forging and hot upsetting processes. In addition, AISI 1045 steel is the focus of many recent studies on numerical modelling of high speed machining process [6–9]. In machining, AISI 1045 steel is characterised by continuous chip formation and it is relatively easier to machine.

Titanium alloys have been widely used in aerospace, biomedical, automotive and petroleum industries because of their good strength-to-weight ratio and superior corrosion resistance. However, the machining of titanium alloys poses a serious challenge for industry due to its tendency to work harden during the machining process, high cutting temperature at the tool–chip interface, high cutting pressures, chatter and its reactivity with the cutting tool materials at more than 500°C. In addition, its low thermal conductivity and low modulus of elasticity impede its machinability [10]. Titanium alloys have high temperature strength which restricts plastic deformation of the metal in shear zone. The thin serrated chips formed during the machining process create small contact area resulting in heat concentration and high stresses at the tool edge. Moreover, its chemical affinity with tool materials during machining leads to adhesion and chemical reaction, promoting tool degradation, which results in poor workpiece surface finish [11]. Titanium alloys are generally difficult to machine at cutting speeds of more than 30 m/min with high speed steel tools and more than 60 m/min with cemented tungsten carbide tools, resulting in very low productivity [12].

1.2 Contact length

In metal cutting, when a continuous chip is formed, it remains in contact with the tool rake face from the cutting edge of the tool over a certain distance known as tool–chip contact length. The tool–chip contact length plays an important role in the metal cutting process. Along with the shear angle, the tool rake face angle and the undeformed

Table 1 Summary of contact length models

Researcher	Contact length model	Workpiece material (cutting speed; m/min)
Lee and Shaffer [18]	$L_c = \frac{h_1\sqrt{2}}{\sin\phi\sin(45^\circ+\phi-\alpha)}$	Mild steel (not specified)
Abuladze [19]	$L_c = 2h_1[\lambda(1-\tan\alpha)+\sec\alpha]$	–[a]
Poletika [20]	$L_c = h_1[2.05\lambda - 0.55]$	Iron[a], steel[a], copper[a], bronze[a]
Kato et al. [21], Toropov and Ko [13]	$L_c=2h_2$	Aluminium, copper, zinc, tin–lead alloy (50), Al 6061 (1,000), Copper (800), AISI 1045 (300), AISI 304 (140)
Tay et al. [22]	$L_c = \frac{h_1\sin\theta}{\cos\alpha\sin\phi}$	AISI 1016 (244)
Vinogradov [23]	$L_c = \frac{h_1\sin\frac{\pi}{4}}{\sin\phi\sin\left(\frac{\pi}{4}+\phi-\alpha\right)}$	–[a]
Oxley [16]	$L_c = \frac{h_1\sin\theta}{\cos\alpha\sin\phi}\left\{1+\frac{C_n}{3\left[1+2\left(\frac{1}{4}\pi-\phi\right)-nC\right]}\right\}$	Low carbon steel −0.16% C (6–60)
Zhang et al. [24].	$L_c = 8.677\times10^{-05}h_1^{0.515}V_c^{-0.065}(90^\circ-\alpha)^{0.733}$	AISI 1045 (300)
Stephenson et al. [17]	$L_c = 0.485 + 0.00280V_c$	AISI 1018 (82)
Marinov [15]	$L_c = 1.61h_2 - 0.28h_1$	AISI 1018 (291)
Sutter [5]	$L_c = 1.92h_2 - 0.09h_1$	XC 18 (3600)

L_c contact length, h_1 undeformed chip thickness, h_2 chip thickness, λ chip compression ratio, α rake angle, ϕ shear angle, V_c cutting velocity, n material constant, C material constant, θ inclination of resultant cutting force to shear plane

[a] Information not available

chip thickness, it defines the geometry of the chip formation zone. Interface friction between the tool and the chip and tool wear takes place along the contact length. Thus, the contact length and the contact area control the amount of heat generation in the secondary deformation zone during the cutting process.

Previous work on contact length has been done on steels, especially low and medium carbon steels [5, 13–17]. Table 1 summarises the contact length models available in literature and the workpiece materials for which these models were developed.

The equations in Table 1 show that almost all of these contact length models are a function of the undeformed chip thickness. Most of these models present tool–chip contact length as a function of the undeformed and the actual chip thickness. The contact length models of Lee and Shaffer [18] and Vinogradov [23] are dependent on shear angle and are very similar in their mathematical form, except for the factor in the numerator. The model of Stephenson [17] is a function of cutting speed only. For a zero cutting velocity, it gives a contact length of 0.485 mm, which is unrealistic. It is assumed that this factor 0.485 is specifically meant for the workpiece tool material combination and cutting conditions used. Oxley's model [16] requires additional data for evaluating 'n' and 'C', which can only be determined experimentally, and for this reason, it is not included in this comparison. Similarly, the model of Tay et al. [22] requires force data for calculating inclination of the resultant cutting force. As cutting forces are not the focus of this study, this model is also not included in the comparison.

Using the split tool method, Kato et al. [21] reported that the contact length is twice the deformed chip thickness. Toropov and Ko [13] concluded the same result using slip line field method. The model by Abuladze [19], for 0° tool rake face angle, becomes similar to models by Kato et al. [21] and Toropov and Ko [13], with a constant factor added to it. Poletika [20], Marinov [15] and Sutter [5] used dimensional analysis to define the contact length for various workpiece materials; due to this reason, their mathematical form is similar as well, though with different coefficients. In addition, the difference in coefficients of Marinov and Sutter contact length models can be attributed to different cutting speeds used (using same workpiece material). This clearly shows the dependence of tool–chip contact length on workpiece material and cutting speed.

Other important factors that may influence the contact length prediction are tool geometry and interface friction. Sutter [5] used different rake angle tools (+5°, 0° and −5°) for contact length measurement and reported large dispersion for normalised contact length. Sutter noted that due to this large dispersion in the results, a clear trend between rake angle and contact length was not obvious. Thus, the model was only developed using the zero degree rake angle contact length data. This approach is however useful, as in machining, once a solid tool or tool holder and insert are selected, then the rake angle is set for the cutting conditions.

Iqbal et al. [25] reported a positive correlation between the interface friction coefficient and contact length when data for various chip compression ratios were considered. If a wide range of cutting speeds is considered (high speed cutting), then reduced friction coefficients are experienced at the higher cutting speeds [26, 27]. Thus, a study of the effect of cutting speed on contact length incorporates friction aspects. This is useful, as in industrial machining, the coefficient of friction is set by the choice of tooling and workpiece materials and then changes with the cutting conditions.

A close look at Table 1 reveals that almost all of the work on estimation of the contact length models is done at low cutting speeds, except Sutter's [5] work. Sutter used a ballistic machining setup to go up to a cutting speed of 3,600 m/min with low carbon steel (~AISI 1018) and uncoated carbide tool. It is also noted that the workpiece materials used in all previous contact length investigations are different grades of steel, copper, bronze and aluminium alloy. As mentioned earlier, AISI 1045 steel, which is the focus of many recent works on numerical modelling of machining, has only been investigated at a maximum cutting speed of 300 m/min. No work on the contact length modelling of Ti6Al4V alloy is reported in literature.

1.3 Scope of current research

Literature review has shown that there are various contact length models available and that these models have not been developed for machining of Ti6Al4V alloy. In addition, these models do not focus on the high speed machining of steels. Thus, there is need to evaluate the applicability of existing contact length models and to further establish more accurate models for the above cases. These models can contribute towards establishing a sound machining process database, especially for the tool–chip contact phenomenon. This is essential for the application of finite element analysis for thermal modelling of the machining process especially at high cutting speeds.

Table 2 Parameters for cutting experiments

Cutting parameter	Work piece material	
	AISI 1045 steel	Ti6Al4V
Cutting speed (m/min)	198 to 879	60 to 300
Undeformed chip thickness (mm)	0.1 to 0.3	0.1 to 0.3
Width of cut (mm)	2.5	2

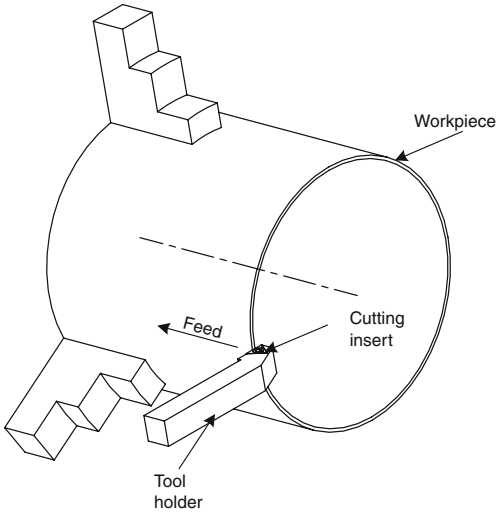

Fig. 2 Schematic of the experimental configuration for the orthogonal cutting tests

2 Experimental details

All the experimental tests were conducted on a commercial lathe machine and under dry conditions (as the benefits of cutting fluids are not so obvious at high cutting speeds [28]). To reduce the variation of cutting speed across the cutting edge, a large diameter workpiece were used. Table 2 summarises the cutting conditions for both workpiece materials.

Commercially available tungsten-based flat triangular uncoated cemented carbide inserts (grade, Sandvik TCMW 16T304 grade 5015) were used in these tests. This insert geometry was selected because it had no chip breaker, thereby not constraining the contact length. During the tests, the inserts were rigidly mounted on right style holder (STGCR 2020K-16), resulting in a 0° rake angle and 7° clearance angle. Cutting tests were performed at different speeds from the conventional to HSM range. The experimental setup is shown in Fig. 2.

For the measurement of the contact length, cutting inserts were examined using a Polyvar optical microscope equipped with image processing software. The contact tracks left by the chip on the tool rake face were utilised for the identification of the contact area.

Table 3 Critical cutting conditions to form shear localised chips

Workpiece material	Thermal conductivity (W/m-K)	fV_c [29]
Ti6Al4V	6.70	0.0040
AISI 304	16.2	0.0054
AISI 4340	44.5	0.0060
AISI 1020	51.9	0.0970

3 Results and discussion

The experimental results for the two workpiece materials are presented in Figs. 3, 6, 7 and 8. These results compare the variation of the contact length and the chip compression ratio with the cutting speed and the undeformed chip thickness.

Figure 3 shows the variation of the contact length with the cutting speed for both workpiece materials. For AISI 1045, the contact length shows a decreasing trend with increasing cutting speed. The same decreasing trend is observed for all undeformed chip thickness values. The contact length increases with the increasing undeformed chip thickness value. For Ti6Al4V alloy (as shown in Fig. 3b), the contact length shows a different trend. Here, the contact length initially increases and then decreases with the cutting speed. The cutting speed of 180 m/min at which the contact length is maximum lies within the transition range between the conventional and high speed machining range for titanium alloys (Fig. 1). This initial increase and then decrease in contact length, for Ti6Al4V alloy at higher feed rates, can be attributed to the phenomena of shear banding.

As mentioned earlier, titanium alloys are characterised by low thermal conductivity, diffusivity and poor machinability. Due to low thermal conductivity, adiabatic shear

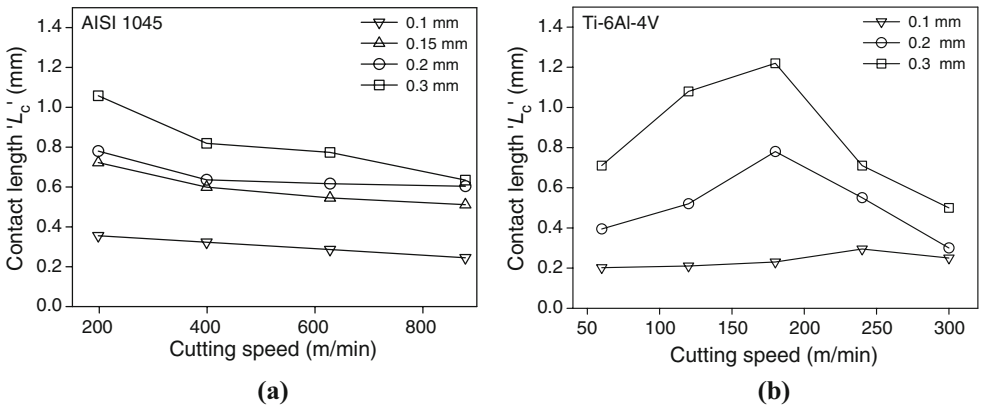

Fig. 3 Variation of contact length with cutting speed for AISI 1045 steel (**a**) and Ti6Al4V alloy (**b**) for various values of undeformed chip thickness

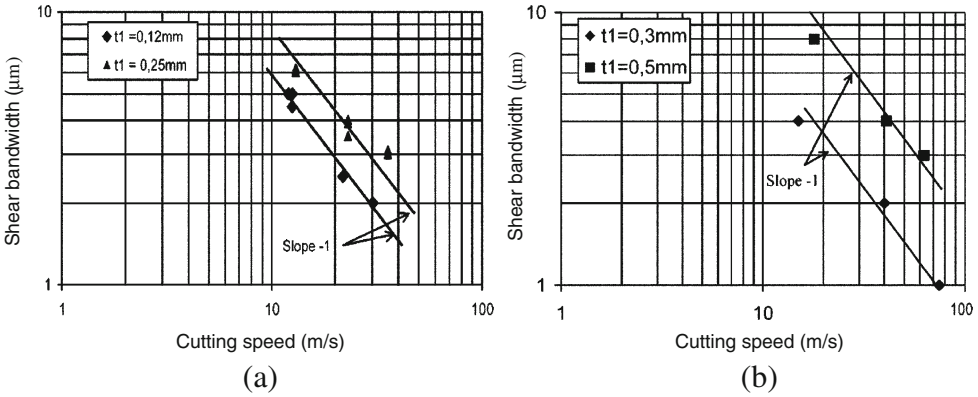

Fig. 4 Adiabatic shear bandwidth as function of cutting speed **a** for Ti6Al4V alloy [28], **b** for medium carbon steel [29]

banding is favoured in this alloy. Chip segmentation by shear localisation occurs in a certain range of cutting velocities. This phenomenon can be desirable in reducing cutting forces and improving chip evacuation. This strain localisation is accompanied by a large local growth of temperature which is a necessary condition to have adiabatic shear bands. Workpiece materials with high thermal conductivity manifest no adiabatic shearing because heat diffusion tends to make the temperature uniform in the specimen.

Bayoumi and Xie [29] studied the effect of the cutting conditions on the formation of shear bands in four different alloys (Ti6Al4V alloy, AISI 304, AISI 4340 and AISI 1020 steel). For each workpiece material considered, there existed a critical value of the product of cutting velocity and feed rate at which shear localised chips were observed. The critical cutting conditions to form shear localised chips for four different workpiece material are given in Table 3, and the thermal conductivity of the workpiece materials is also added to aid the discussion. The values for parameter 'fV_c' listed in the table suggest that the shear banding frequency increased with an increase in feed rate or a decrease in cutting speed.

AISI 1020, which is close to AISI 1045 as compared to all other materials, has the highest value of thermal conductivity and highest parameter 'fV_c'. This implies that shear banding will occur at far higher cutting speeds for steel compared to titanium alloys. This supports a decreasing trend of contact length at the transition to HSM cutting speeds as shown in Fig. 3a for AISI 1045 in comparison to Ti6Al4V alloy in Fig. 3b.

For higher cutting speeds, Molinari et al. [30] discussed the phenomena of adiabatic shear banding of Ti6Al4V alloy and used two cutting speed ranges (0.6 to 72 m/min and 600 to 4380 m/min). Molinari et al. did not report any experimental results between cutting speed range of 72 to 600 m/min. They suggested that for titanium alloys with cutting velocities lower than 72 m/min, that chip serration was related to the development of deformed shear bands, which are the manifestation of thermo-mechanical instability. However, at these low values of the cutting velocity, the instability process is weak and the localisation is not sharp as for high cutting velocities. For cutting velocities higher than 720 m/min, the adiabatic shear bands had marked boundaries and seemed to be transformed bands in which phase change had occurred. They have reported that shear bandwidth decreases with increasing cutting speed. In addition, the width of shear band increases with increasing feed rate for Ti6Al4V, as shown in Fig. 4a.

Sutter et al. [31] performed similar experimental investigation using plain carbon steel for very high cutting speeds and reported similar trend for shear bandwidth (as

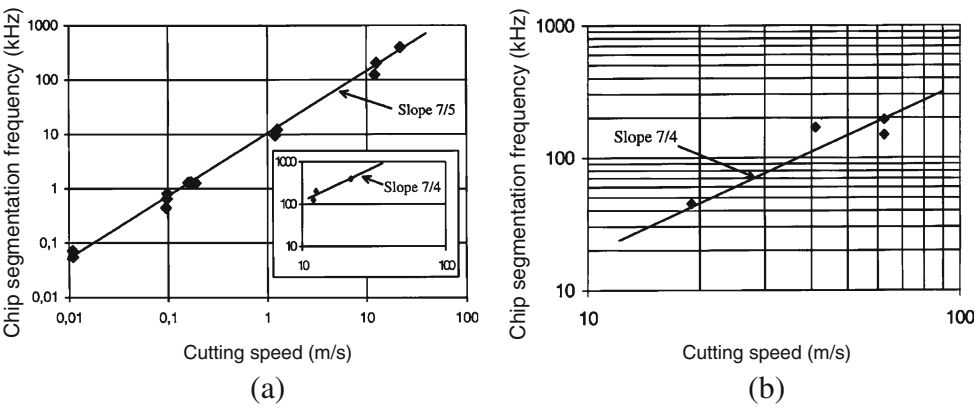

Fig. 5 Frequency of chip segmentation for α=0° as function of cutting speed **a** for Ti6Al4V alloy [28], **b** for medium carbon steel [29]

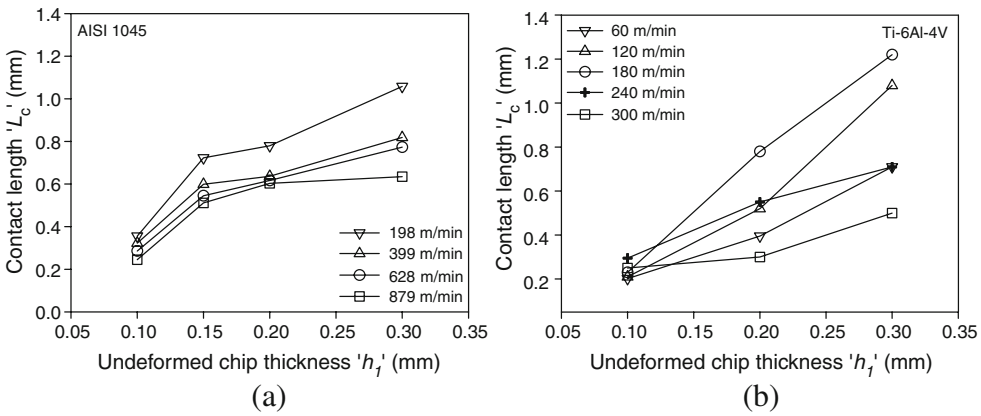

Fig. 6 Variation of contact length with undeformed chip thickness for AISI 1045 steel (**a**) and Ti6Al4V alloy (**b**) for a range of cutting speeds

shown in Fig. 4b), but for higher cutting speeds with higher feed rates, as compared to titanium alloy. Similarly, the frequency of chip segmentation increased with increasing cutting speed for both workpiece materials, as shown in Fig. 5a and b. From this figure, the chip segmentation frequency for plain carbon (reported by Sutter et al. [31]) was around 20 kHz as compared to 300 kHz for titanium alloy (reported by Molinari et al. [30]) at the same cutting speed (600 m/min).

Molinari et al. reported that the phenomenon of adiabatic shear banding is weak and not established at low cutting speed. This might be responsible for the increased contact length at low cutting speeds (as reported in Fig. 3b). In addition, increased chip segmentation frequency (established shear bands) can support reduction in contact length at higher cutting speed as reported for titanium alloys (Fig. 3b). Moreover, it also supports less deterministic trend for contact length for titanium alloy compared to steel, and hence high scatter in contact length data.

Nuri et al. [32, 33] reported a trend of increase in contact length for cutting speed greater than 400 m/min after an initial decrease. The workpiece material used was AISI 4140 steel with uncoated and different coated carbide tools. The cutting speeds range used was 200 and 1,200 m/min. According to Table 3, the parameter 'fV_c' for AISI 4340 steel (which is close to AISI 4140 steel) is high as compared Ti6Al4V alloy. In the light of above discussion and results reported in Figs. 3a and b, 4a and b, 5a and b and Table 3, it might be possible for the contact length to increase for AISI 1045 steel beyond the cutting speeds reported in this study.

Figure 6 shows the contact length variation with the undeformed chip thickness. For both workpiece materials, the contact length increases with the increasing value of undeformed chip thickness. A similar trend was reported by Sadik and Lindstrom [34] for turning SS1572 (0.35% C, quenched and tempered) steel, by Marinov [15] for turning AISI 1020 at low cutting speeds and by Sutter [5] for cutting XC18 (0.18% C) steel at very high speeds using ballistic machining setup. For AISI 1045 steel, at high cutting speeds, the contact length appears to be insensitive to undeformed chip thickness. For Ti6Al4V alloy, the contact length variation shows an increasing trend with a steep slope at the cutting speeds of 120 and 180 m/min. For the other three cutting speeds, i.e. 60, 240 and 300 m/min, the increase in contact length is low. It is interesting to note that cutting speeds of 120 and 180 m/min fall within the transition cutting speed range for titanium alloys (Fig. 1). However, the effect of transition cutting speed range is not pronounced for AISI 1045 steel. As discussed earlier, it

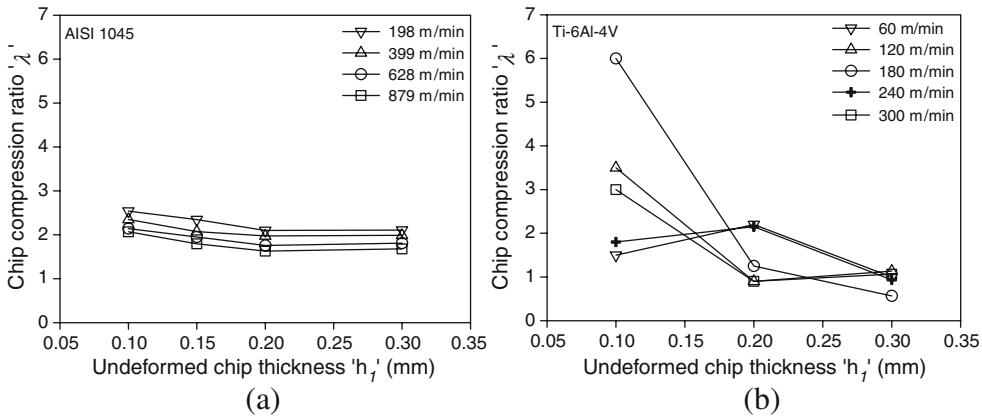

Fig. 7 Variation of chip compression ratio with undeformed chip thickness for AISI 1045 steel (**a**) and Ti6Al4V alloy (**b**) for a range of cutting speeds

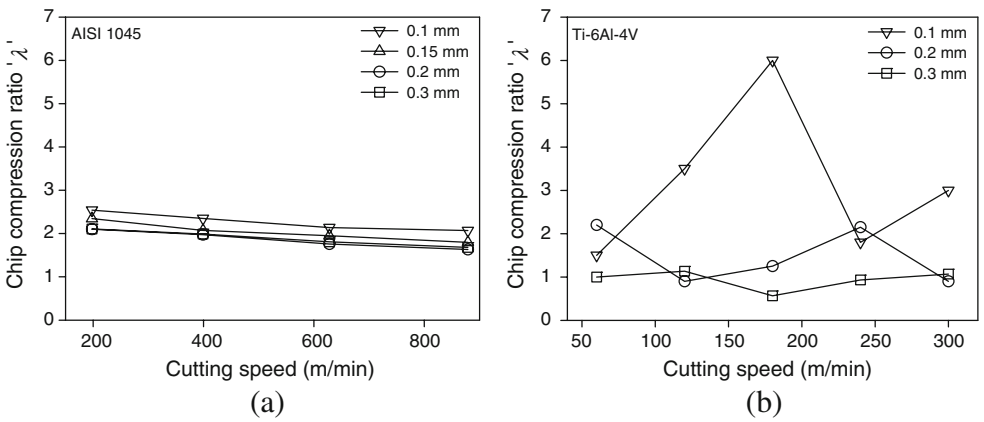

Fig. 8 Variation of chip compression ratio with cutting speed for AISI 1045 steel (**a**) and Ti6Al4V alloy (**b**) for various values of undeformed chip thickness

might be attributed to the phenomena of chip segmentation. It is also noted that the changes in the contact length for various cutting speeds are more pronounced for higher feed rates. This appears reasonable, as at higher feed rates, increased chip thickness and cutting forces are encountered. Thicker chips are more difficult to deform and hence associated with increased contact length.

Chip compression ratio is an important parameter in evaluating the heat flux and approximating the degree of deformation during machining process. It is a measure of the efficiency of chip formation [3]. A lower value of chip compression ratio leads to higher shear angle, which, in turn, leads to lower strain in the chip and reduced energy consumption. Chip compression ratio can be defined by Eq. 1 as:

$$\lambda = \frac{h_2}{h_1} \tag{1}$$

where h_1 is the undeformed chip thickness (set by the feed rate in the depicted orthogonal turning) and h_2 is the actual chip thickness.

Figure 7 shows the variation of the chip compression ratio with the undeformed chip thickness. For AISI 1045, the chip compression ratio follows a decreasing trend with increasing undeformed chip thickness. The chip compression ratio is a crude estimate of the amount of strain experienced in machining. This implies that in this case, strain inducing mechanisms are more prevalent when taking lighter cuts (HSM is typically done at lighter cuts). In addition, the chip compression ratio decreases with increasing cutting speed. The chip compression ratio for all the cutting speeds used follows a consistent and even trend. However, for Ti6Al4V alloy, the chip compression ratio shows two distinct trends for the five cutting speeds used. For the cutting speeds of 120, 180 and 300 m/min, the chip compression ratio shows a decreasing trend with increasing undeformed chip thickness. Furthermore, the chip compression ratio drops drastically for undeformed chip thickness from 0.1 to 0.2 mm. For the cutting speed of 60 and 240 m/min, there is a slight increase in chip compression ratio at undeformed chip thickness of 0.2 mm, and then it finally decreases. The chip compression ratio values at the undeformed chip thickness of 0.3 mm are very close for all cutting speeds used.

Figure 8 shows the variation of chip compression ratio with the cutting speed. Again, for AISI 1045 steel, the variation of the chip compression ratio shows a decreasing trend with increasing cutting speed within a narrow band and without any scatter, whereas for Ti6Al4V alloy, at undeformed chip thickness of 0.1 mm, the chip compression ratio increases until the cutting speed of 180 m/min. After that, there is a sharp drop in the chip compression ratio at the cutting speed of 240 m/min, but it starts to increase again at the cutting speed of 300 m/min. The scatter in the chip compression ratio with increasing speed

Table 4 Dimensional analysis of tool–chip contact length

Parameter	Symbol	Dimension
Tool–chip contact length	L_c	Length
Tool's rake face angle	α	–
Undeformed chip thickness	H_1	Length
Chip thickness	H_2	Length

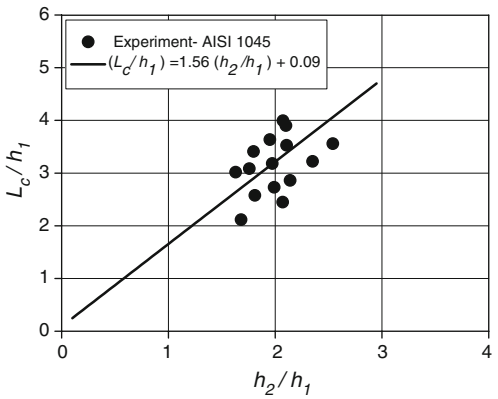

Fig. 9 Experimental results for the tool–chip contact and proposed contact length model (Eq. 3) for AISI 1045 steel

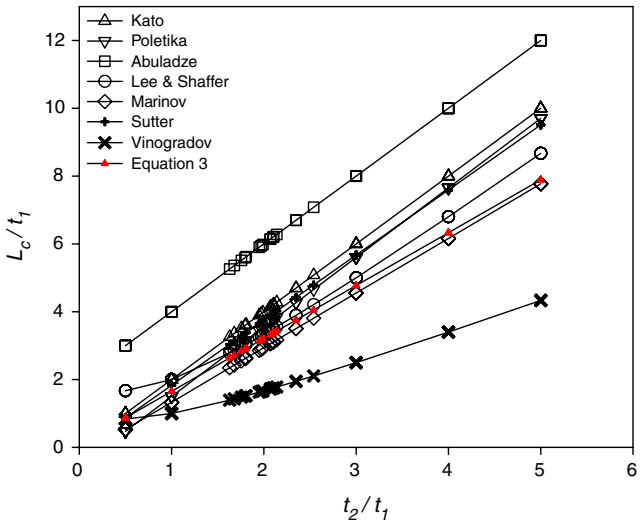

Fig. 10 Comparison of various tool–chip contact length models with the contact length model (Eq. 3) obtained in the present work for AISI 1045 steel

is not high for undeformed chip thickness value of 0.2 and 0.3 mm.

4 Dimensional analysis

A dimensional analysis, similar to the one reported by Marinov [15], is performed to identify the cutting parameters which strongly influence the tool–chip contact length. For a given combination of tool and workpiece material, three quantities in addition to L_c are necessary to completely define the geometry of the chip formation zone: the tool rake face angle 'α', the undeformed chip thickness 'h_1' and the actual chip thickness 'h_2'. In the case of two-dimensional orthogonal cutting, the width of cut does not affect the geometry of the chip formation. Cutting velocity 'V_c' is known to change the chip–tool contact length and the shear angle, but only indirectly, through its influence on the cutting temperature and hence the work material properties.

The main parameters which are involved in the determination of L_c are those listed in Table 4. The normalised tool–chip contact length as a function of the undeformed chip thickness 'h_1' and the actual chip thickness 'h_2' is given by:

$$\frac{L_c}{h_1} = f\left(\frac{h_2}{h_1}\right) \tag{2}$$

where $\frac{L_c}{h_1}$ is the normalised contact length and $\frac{h_2}{h_1}$ is the chip compression ratio.

Figure 9 shows the experimental results for AISI 1045 steel. These results are correlated with a coefficient of correlation of 0.84 and a coefficient of determination of 0.71. The linear equation defining the contact length for AISI 1045 for a wide range of cutting speeds is obtained as:

$$L_c = 1.56h_2 + 0.09h_1 \quad \text{(AISI 1045 steel)}. \tag{3}$$

Figure 10 shows the variation of normalised contact length (Eq. 3) with the chip compression ratio for AISI 1045 steel, along with other contact length models presented in Table 1, covering a wide range of cutting speeds. As mentioned earlier, for 0° tool rake face angle, the contact length models by Abuladze [19], Kato et al. [21] and Toropov and Ko [13] turns out to be the same; hence, they overlap. In addition, the contact length models by Oxley [16] and Tay et al. [22] require additional input parameters to define contact length, so they are excluded from this discussion. The proposed contact length model given by Eq. 3 shows that 'L_c' tends near to zero as the chip compression ratio 'h_2/h_1' approaches zero. The Marinov's model [15], based on the same formulation, has a similar slope to that of Eq. 3 but a different intercept. The new model has an intercept value closer to zero, thus representing a more realistic case for machining. The slope of Poletika model [20] is steeper as compared to the new model (Eq. 3) and so is that of Sutter's model [5]. Lee and Shaffer's model [18], which is strongly dependent on the shear angle and in turn on chip compression ratio, is closest

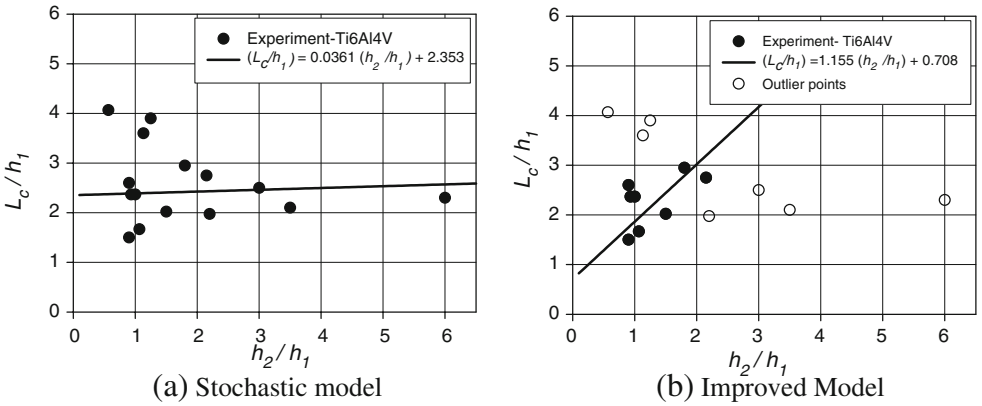

Fig. 11 Experimental results for the tool–chip contact and proposed contact length model for Ti6Al4V alloy

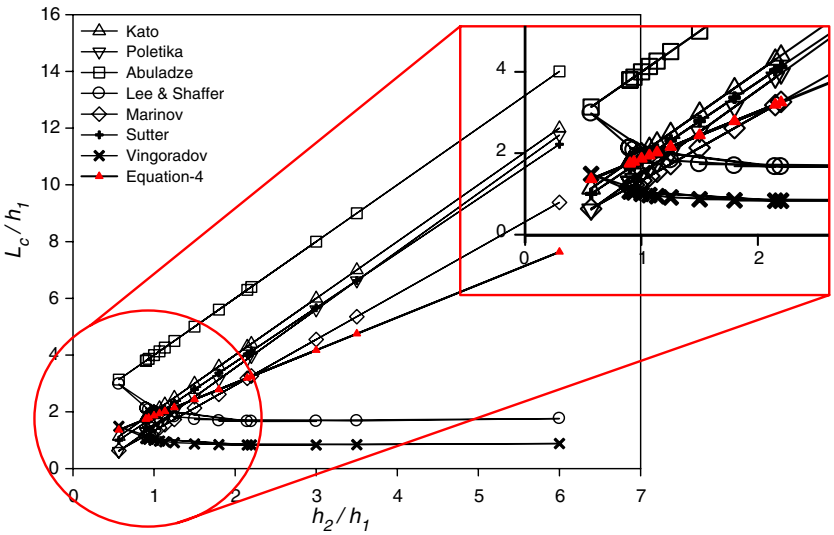

Fig. 12 Comparison of various tool–chip contact length models with the contact length model (Eq. 4) obtained in the present work for Ti6Al4V alloy

to Eq. 3. This might be due to a very small scatter in the experimental data points for chip compression ratio, as shown in Figs. 7 and 8. On the other hand, Vinogradov's model [23], which is very similar in mathematical form to Lee and Shaffer's model, provides a more conservative estimate of contact length as compared to the new model (Eq. 3). The models by Kato et al. [21], Toropov and Ko [13] and overestimate contact length compared to Eq. 3, whereas contact length predicted by Abuladze's [19] model overestimates Eq. 3 by a large margin.

Figure 11a shows the experimental results for normalised contact length and chip compression ratio of Ti6Al4V alloy. Due to the poor machinability characteristics of Ti6Al4V alloy and resulting high degree of scatter in contact length data, the linear equation fitted has very low coefficient of correlation value of 0.053. The resulting linear equation gives a normalised contact length of 2.35 at zero chip compression ratio. This would suggest that predicting contact length for titanium alloys is severely changed by the material behaviour.

After excluding outlier data points using statistical analysis technique (based on minimising the standard error of mean), the experimental results are correlated with a coefficient of correlation of 0.79 and a coefficient of determination of 0.62. The linear equation (as shown in Fig. 11b) for contact length in this case is obtained as shown in Eq. 4.

$$L_c = 1.15h_2 + 0.70h_1 \quad \text{(Ti6Al4V alloy)} \tag{4}$$

Figure 12 shows the variation of normalised contact length model, given by Eq. 4 with the chip compression ratio for Ti6Al4V alloy, along with other contact length models presented in Table 1, covering a wide range of cutting speeds. The models by Lee and Shaffer [18] and Vinogadov [23] show similar trends and are different from all other contact length models. The normalised contact length predicted by these models is almost constant for increasing chip compression ratio. It is noted that the form of these contact length models (Table 1) is similar and is strongly dependent on shear angle 'ϕ', which, in turn, is dependent on the chip compression ratio 'h_2/h_1'. From Fig. 7, the chip compression ratio for Ti6Al4V alloy shows a larger scatter as compared to AISI 1045 steel. For the rest of the contact length models, the normalised contact length shows an increasing trend with increasing ratio of 'h_2/h_1'. The model given by Eq. 4 has a different slope than the rest of the models. This is due to the fact that the experimental basis for all the contact length models presented in Table 1 are mostly for different grades of steel as the workpiece material. Due to poor machinability of titanium alloys and the resulting large scatter of the experimental data, the

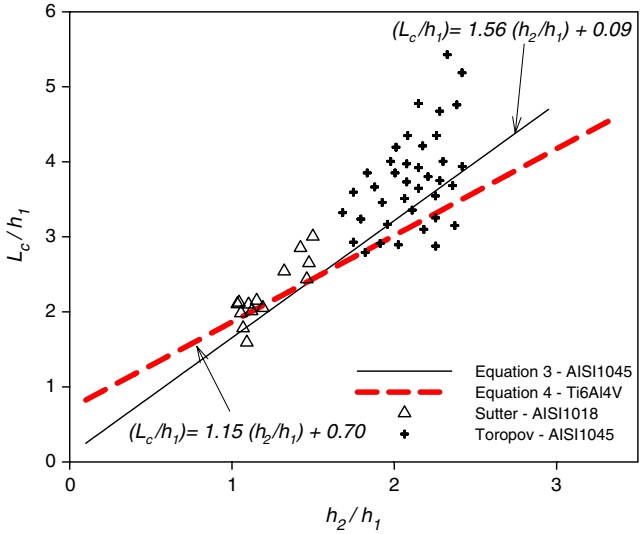

Fig. 13 Comparison of proposed contact length models with reported experimental data

contact length relation given by Eq. 4 gives deviation from zero when ratio 'h_2/h_1' reduces to zero.

Figure 13 shows the comparison of the proposed contact length models (Eqs. 3 and 4) with other reported experimental results. The experimental tool–chip contact length data for Ti6Al4V are not reported in literature. The experimental data selected here for comparison are reported by Toropov and Ko [13] (AISI 1045 steel, V_c=80 to 300 m/min, h_1=0.1 to 0.25 mm, tool rake face angle=−5° and 20°, h_2/h_1>1.75, tool: uncoated cemented carbide) and Sutter [5] (~AISI 1018 steel, V_c=1,020 to 3,600 m/min, h_1=0.02 to 0.65 mm, tool rake face angle=0°, h_2/h_1<1.75, tool: uncoated cemented carbide). These two experimental data sets cover a wide range of cutting speeds, i.e. from 80 to 3,600 m/min. Toropov's experimental data points are more towards high normalised contact length and slightly overestimate Eq. 3 (AISI 1045 steel). The experimental data reported by Toropov are for four different rake angles (−5°, 0°, 10°, 20°), and the upward shift in these data may be attributed to this. The results reported by Sutter were obtained at 0° tool rake angle and for very high cutting speeds (ballistic cutting setup used). The experimental data points are on the upper side of proposed contact length model (Eq. 3).

5 Conclusions

Contact length models provide an estimate for the size of the zone for heat transfer from the chip to the tool. Whilst a number of models have previously been developed for predicting contact length, these were not developed and tested for titanium alloys for high speed machining. Deformed and undeformed chip thickness values are important in predicting contact length. This study has sought to clarify how material differences can affect tool–chip contact length. For AISI 1045 steel, a decreasing trend is observed for the contact length with increasing cutting speed for all undeformed chip thickness values. For Ti6Al4V alloy, a noticeable rise in the tool–chip contact length is observed at cutting speeds which have, in the past, been categorised as the transition range before HSM range. This can be attributed to the phenomena of adiabatic shear banding occurring in low thermal conductivity and diffusivity materials. It is also shown that the chip compression ratio has a high degree of scatter for titanium alloy compared to steel, and this can be attributed to the poor machinability characteristics and phenomena of shear banding of the former. Review of the existing contact length models has highlighted their inadequacy in accurately providing a quantitative prediction of contact length for the cases considered. Two new contact length models have been proposed based on dimensional analysis of the contact zone parameters. These new models cover a wide range of cutting speeds and have a higher coefficient of determination than reported previously in literature. Additionally, the study shows that the predictive capability of contact length models is affected by the deterministic nature of workpiece material machinability.

Acknowledgement The authors wish to acknowledge the background work done by Mark Hinchliffe and Mehrban Hussain in the machinability of titanium of alloy.

References

1. Schulz H, Moriwaki T (1992) High speed machining. Ann CIRP 41(2):637–644
2. Denkena B, Amor RB León-García Ld, Dege J (2006) Material specific definition of the high speed cutting range. Fifth International Conference on High Speed Machining, Metz, France, pp 1–12
3. Flom DG, Komanduri R, Lee M (1984) High speed machining of metals. Annu Rev Mater Sci 14:231–278
4. Schulz H (2001) Scientific fundamentals of HSC. Hanser, Munich, pp v–vi
5. Sutter G (2005) Chip geometries during high speed machining for orthogonal cutting conditions. Int J Mach Tools Manuf 45(6):719–726
6. Grzesik W (2006) Determination of temperature distribution in the cutting zone using hybrid analytical-FEM technique. Int J Mach Tools Manuf 46(6):651–658
7. Klocke F, Raedt H-W, Hoppe S (2001) 2D-FEM Simulation of the orthogonal high speed cutting process. Min Sci Technol 5(3):323–340
8. Ivester RW, Kennedy M, Davies M, Stevenson R, Thiele J, Furness R et al (2000) Assessment of machining models: progress report. Min Sci Technol 4(3):511–538
9. Xie L-J, Schmidt J, Schmidt C, Biesinger F (2005) 2D FEM estimate of tool wear in turning operation. Wear 258:1479–1490
10. Ezugwu EO, Wang ZM (1997) Titanium alloys and their machinability—a review. J Mater Process Technol 68:262–274
11. Cherukuri R, Molian P (2003) Lathe turning of titanium using pulsed laser deposited, ultra hard boride coating of carbide inserts. Min Sci Technol 7(1):119–135
12. Rahman M, Wang Z-G, Wong Y-S (2006) A review on high-speed machining of titanium alloys. Mechanical systems. Mach Elem Manuf 49(1):11–20
13. Toropov A, Ko S-L (2003) Prediction of tool–chip contact length using a new slip-line solution for orthogonal cutting. Int J Mach Tools Manuf 43:1209–1215
14. Friedman MY, Lenz E (1970) Investigation of the tool–chip contact length in metal cutting. Int J Mach Tools Des 10:401–416
15. Marinov V (1999) The tool chip contact length on orthogonal metal cutting. 5th International Conference on Advanced Engineering and Technology, AMTECH 99, Plovdiv, Bulgaria, pp 149–155
16. Oxley PLB (1989) Mechanics of machining: an analytical approach to assessing machinability. Ellis Horwood, London
17. Stephenson DA, Jen T-C, Lavine AS (1997) Cutting tool temperature in contour turning: transient analysis and experimental verification. Trans ASME J Manuf Sci Eng
18. Lee EA, Shaffer BW (1951) The theory of plasticity applied to a problem of machining. Trans ASME J Appl Mech 18:405–413
19. Abuladze NG (1962) Character and the length of tool–chip contact (Russian). Machinability of heat-resistant & titanium alloys. Kuibyshev, pp 68–78

20. Poletika MF (1969) Contact loads on tool faces (Russian). Machinostronie, Moscow
21. Kato S, Yamaguchi K, Yamada M (1972) Stress distribution at the interface between tool and chip in machining. Trans ASME J Eng Ind 94:683–689
22. Tay AO, Stevenson MG, de Vahl G (1976) A numerical method for calculating temperature distribution in machining from force and shear angle measurement. Int J Mach Tool Des Res 16:335–349
23. Vinogradov AA (1985) Physical foundations of the process of drilling difficult-to-cut materials using carbide drills. Naukova Dumka, Kiev
24. Zhang HT, Liu PD, Hu RS (1991) A three-zone model and solution of shear angle in orthogonal machining. Wear 143:29–43
25. Iqbal SA, Mativenga PT, Sheikh MA (2008) Contact length prediction: mathematical models and effect of friction schemes on FEM simulation for conventional to HSM of AISI 1045 steel. Int J Machinability Machining Mater 3(1/2):18–33
26. Devillez A, Lesko S, Mozerc W (2004) Cutting tool crater wear measurement with white light interferometry. Wear 256(1–2):56–65
27. Iqbal SA, Mativenga PT, Sheikh MA (2007) Characterization of the machining of AISI 1045 steel over a wide range of cutting speeds—Part 1: Investigation of contact phenomena. Proc IMechE Part B: J Eng Manuf 221(5):909–916
28. Dudzenski D, Devillez A, Moufki A, Larrouquere D, Zerrouki V, Vigneau J (2004) A review of developments towards dry and high speed machining of Inconel 718 alloy. Int J Mach Tools Manuf 44:439–456
29. Bayoumi AE, Xie JQ (1995) Some metallurgical aspects of chip formation in cutting Ti–6wt.%Al–4wt.%V alloy. Mater Sci Eng A 190:173–180
30. Molinari A, Musquar C, Sutter G (2002) Adiabatic shear banding in high speed machining of Ti-6Al-4V: experiments and modelling. Int J Plast 18(4):443–459
31. Sutter G, Faure L, Molinari A, Delime A, Dudzinski D (1997) Experimental analysis of the cutting process and chip formation at high speed machining. J Phys IV 7:33–38
32. Abukhshim NA, Mativenga PT, Sheikh MA (2004) An investigation of the tool–chip contact length and wear in high-speed turning of EN19 steel. Proc. Inst Mech. Eng Vol. Part B J. Eng Manuf 218:889–903
33. Abukhshim NA, Mativenga PT, Sheikh MA (2006) Tool–chip contact phenomena for uncoated and coated carbides in high speed turning of high strength alloy steel. 5th International Conference on High Speed Machining. Metz, France, pp 1–10
34. Sadik MI, Lindstrom B (1993) The role of tool–chip contact length in metal cutting. J Mater Process Technol 37:613–627